pISSN 1229-3008 eISSN 2287-6251
Progress in Superconductivity and Cryogenics
Vol.20, No.4, (2018), pp.20~25 https://doi.org/10.9714/psac.2018.20.4.020

Line-shaped superconducting NbN thin film on a silicon oxide substrate

Jeong-Gyun Kim[a], Dongseok Suh[a], and Haeyong Kang[b,*]

[a] *Department of Energy Science, Sungkyunkwan University, Suwon 16419, Republic of Korea*
[b] *Department of Physics, Pusan National University, Busan 46241, Republic of Korea*

(Received 16 November 2018; revised or reviewed 27 December 2018; accepted 28 December 2018)

Abstract

Niobium nitride (NbN) superconducting thin films with the thickness of 100 and 400 nm have been deposited on the surfaces of silicon oxide/silicon substrates using a sputtering method. Their superconducting properties have been evaluated in terms of the transition temperature, critical magnetic field, and critical current density. In addition, the NbN films were patterned in a line with a width of 10 μm by a reactive ion etching (RIE) process for their characterization. This study proves the applicability of the standard complementary metal–oxide–semiconductor (CMOS) process in the fabrication of superconducting thin films without considerable degradation of superconducting properties.

Keywords: niobium nitride, superconducting thin film, sputtering deposition, Ar Etching. Critical Temperature, critical field, critical current density

1. INTRODUCTION

Niobium nitride (NbN) is one of the most extensively investigated superconducting materials with excellent physical properties, including a high-critical temperature (T_C), and high-critical magnetic field (H_C). These features promote its potential use in a variety of technical applications in micro–nano devices [1-4]. T_C values as high as 17 K have been reported for bulk NbN samples, however, the corresponding values for thin films tend to be lower. In general, the NbN film is polycrystalline and exhibits various crystallinity depending on the relative ratio between Nb and N [5-7]. Among the various existing NbN phases, δ–NbN has been known to have a high T_C value of the order of ~16 K. Thus, it is important to control the ratio between Nb and N because it affects the superconducting properties according to its composition.

High-quality superconducting films are usually obtained by epitaxial growth. Hence, it is effective to use a substrate which has a similar lattice structure with the material that will be grown on that substrate [8]. In the case of NbN, the MgO substrate is mainly used to get high transition temperature [9-12]. Another way to improve the quality of the film is the inclusion of a heating process because it induces better crystallization owing to high-temperature deposition [13-15]. In general, NbN does not elicit superconducting properties when it is deposited at room temperature but undergoes superconducting transition in high-temperature depositions (several hundred degrees Celsius). However, a choice of the specific substrate or a high-temperature process interrupt the various applications of NbN. Specially, high deposition temperature becomes a drag on patterning the film in micro-nano scale by the typical lithography techniques using organic materials, such as electron-beam/photo resist because the organic resist is decomposed at high temperatures.

A high-quality superconducting film at the micro–nano scale can be employed for various applications. For example, it can be used as a constituent of a superconducting hot electron bolometer mixer [16, 17], or for a superconducting single-photon detector [18-22], which is a very sensitive photon detector by measuring the effect of a chain of superconducting breakdown. Furthermore, a flexible superconducting yarn can be fabricated by the deposition of an NbN thin film on the functional substrate, such as the aligned arrays of carbon nanotube sheets [23, 24]. Herein, we report the superconducting properties of a sputter-deposited NbN thin film on the surface of a SiO_2/Si substrate. The superconducting properties for the various NbN thin film samples with different thicknesses have been compared, and the possibilities of patterning these films have been examined by the patterning of thin line shapes of NbN thin films.

2. EXPERIMENTAL SECTION

NbN films were deposited in a mixture gas of Ar and N_2 (ratio of Ar/N_2: 99/1) using a Nb target (purity 99.98 %, 46 mm diameter, Process Materials Inc., USA) using radio frequency sputtering. The base pressure of the sputter system was 8.5×10^{-7} Torr, and the deposition was performed at a working pressure of 2 mTorr. The films were deposited on commercially available SiO_2/Si substrates at 600 ℃. The applied power was 320 W (~0.28 nm/s) and the thickness was varied from 50 nm to 400 nm by controlling the operating time.

* Corresponding author: haeyong.kang@pusan.ac.kr

TABLE 1
COMPARISON OF CRITICAL TEMPERATURE OF NBN THIN FILMS UNDER VARIOUS DEPOSITION CONDITIONS.

	Substrate	Deposition Temperature	NbN Thickness	Critical Temperature
Ref. 1	3 *C*-SiC/Si	800 °C	5 nm	11.3 K
Ref. 16	3 *C*-SiC/Si	800 °C	4 nm	11.8 K
Ref. 11	MgO	600 °C	200 nm	15.5 K
Ref. 10	Graphene on SiO_X/Si	600 °C	250 nm	~ 14 K
Ref. 26	SiO_X/Si	600 °C	400 nm	~ 14 K (14.8 K onset)
Our Sample	SiO_2/Si	600 °C	400 nm	~ 13.8 K

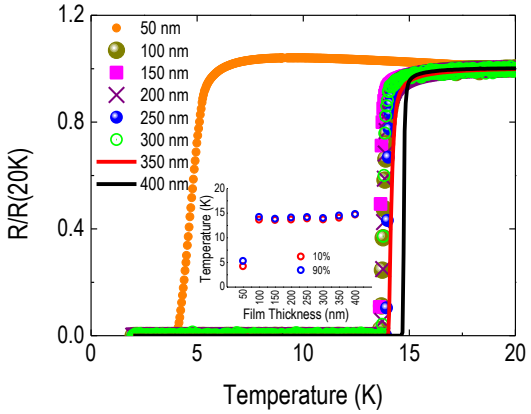

Fig. 1. Temperature dependence curves of normalized resistance for different NbN film thicknesses. The inset data shows the values of critical temperature, $T_{90\%}$, and $T_{10\%}$. These are defined as the values at $R(T_{90\%})$ = 0.9R(20 K), and $R(T_{10\%})$ = 0.1R(20 K), respectively.

After the deposition of the NbN film, patterning was required to accurately measure the critical current density (J_C). We could not process the pattern by lithography using general polymers because of the high deposition temperature above operating temperature of organic polymers. Therefore, after the NbN film was deposited on the substrate with the dimensions of 1.2 cm × 1.2 cm, a RIE process using Ar gas proceeded to remove other parts except a final line pattern. Negative photoresist (AZ5214) was used to cover and protect the lined shape from etching and then was removed after etching process. Finally, we could make a patterned film with dimensions of 10 μm (width) × 1 cm (length).

To evaluate superconducting properties, the general four-probe method for resistance measurement was adopted as the temperature changed from 2 K to 300 K, and the magnetic field from 0 T to 14 T using a physical property measurement system (PPMS Dynacool, Quantum Design Inc., USA).

3. RESULTS AND DISCUSSION

We have made various attempts to determine the optimal conditions for the NbN film deposition process. The ratio of the Ar/N_2 gas mixture and the deposition temperature were paid particular attention to because they play a crucial role in determining the composition of NbN that will be crystallized. After the films were deposited under the various combinations of the ratio of the mixed gas and the deposition temperature, the electrical measurements and analysis according to each condition were followed to select the best condition. Throughout this paper, the films were grown on the SiO_2/Si substrate with the mixed gas ratio of Ar 99 % and N_2 1 % at 600 °C. It is worth mentioning that we primarily focused on the identification of the right condition to apply the superconducting film in a variety fields other than to improve outstanding superconducting properties.

Fig. 1 shows the superconducting transition temperature at different film thickness with full coverage on a SiO_2/Si substrate. The thickness values of the NbN films varied from 50 nm to 400 nm at 50 nm intervals. The resistance of each sample was measured while the temperature decreased from 300 K to 2 K. The transition temperature varied according to its thickness from a T_C of 14.6 K for a 400 nm film to a T_C of 13 K for a 100 nm film. In addition, for film thicknesses higher than 100 nm, films yielded a phase transition phenomenon with a steep resistance change within ~0.7 K. In contrast, we observed a sudden decrease in T_C at a film thickness of 50 nm, where the phase transition started at 5.5 K and exhibited a relatively broader transition. Rapid reduction of the transition temperature below a certain thickness is often seen in superconducting films deposited on lattice-mismatched substrate [25].

The growth conditions and the quality of NbN films were compared with those of other NbN films in Table 1. Superconducting properties of the NbN thin films manifested in the different thickness and various kinds of substrate. In [1], [11] and [16], a film with high-crystallinity grown according to an elaborate effort yields a high-critical temperature, even in a few tens of nanometers thick layer. Meanwhile, using easy accessible deposition conditions and SiO_2/Si substrate like [10], [26], and our sample, the superconducting transition occurred at a comparable high temperature. This provides credible evidence that NbN thin films can combine with various materials while exhibiting quite robust superconductivity.

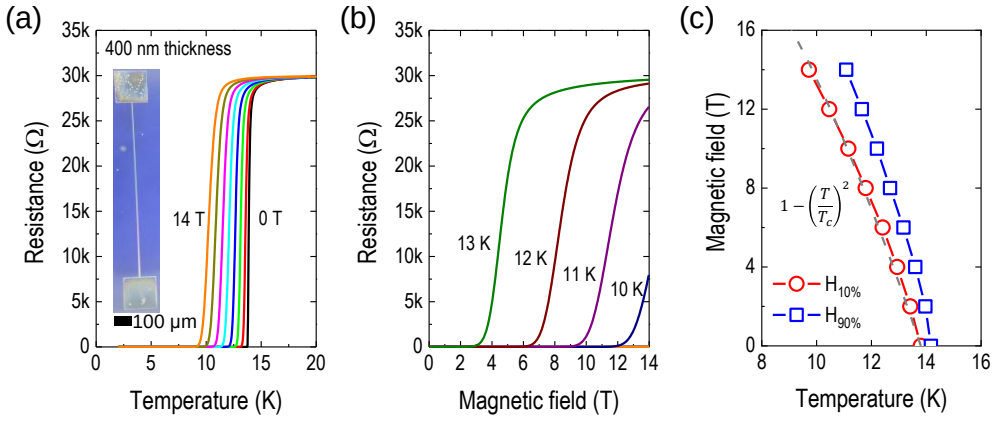

Fig. 2. Superconducting properties of NbN-patterned film with a thickness of 400 nm. (a) Temperature dependence of resistance at different magnetic fields. The inset image shows a patterned film with dimensions of 10 μm (width) × 1 cm (length) × 400 nm (thickness). (b) Magnetic field dependence of resistance at different temperatures. (c) *H-T* phase diagram for a 400nm thick NbN film. The two values of critical magnetic field, $H_{90\%}$ and $H_{10\%}$, are defined as the values at $R(H_{90\%}, T) = 0.9R(20\ \mathrm{K})$ and $R(H_{10\%}, T) = 0.1R(20\ \mathrm{K})$, respectively.

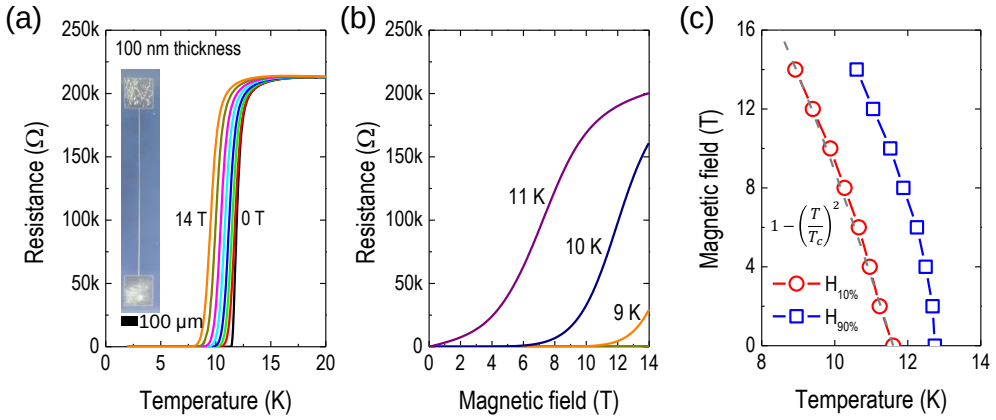

Fig. 3. Superconducting properties of NbN-patterned film with a thickness of 100 nm. (a) Resistance as a function of temperature at different magnetic fields. The inset shows the optic image of a patterned film with 10 μm (width) × 1 cm (length) × 100 nm (thickness). (b) Magnetic field dependence of resistance at different temperatures. (c) *H-T* phase diagram for a 100nm thick NbN film. The same definition as Fig.2 is used for critical magnetic fields.

To analyze the characteristics of superconductivity, it is important to test T_C, H_C, and the critical current (I_C). However, because NbN has a high I_C, it is necessary to use a bar-shaped sample with dimensions of the order of μm in order to obtain a measurable current value at the laboratory scale. Therefore, the geometrical dimension of the film was reduced by an additional RIE process as described in the experimental section (insets of Fig. 2(a) and Fig. 3(a)). The characteristics of all patterned samples were evaluated under various temperatures, magnetic fields, and currents.

Fig. 2 shows the resistance change as a function of temperature and the magnetic field of a 400 nm thick patterned film. Fig. 2(a) shows a zero resistance at 13.8 K at 0 T. However, when the magnetic field increases by 2 T, the T_C decreases systematically according to the magnitude of the magnetic field, and has a value of approximately 8.9 K at 14 T. In Fig. 2(b), superconductivity begins to break at 2.3 T at 13 K near the transition temperature, and H_C rapidly increases as a function of decreasing temperature. When the temperature is lower than 9 K, the value of the H_C of the NbN film cannot be measured because of the limited value of the magnetic field that can be applied. That is, below a temperature of 9 K, the superconducting characteristic is maintained even when a magnetic field of 14 T is applied to the sample. The outstanding field properties of the NbN films are shown in Fig. 2(c). Fig. 2(c) shows the values of temperature and magnetic field where the sample resistance reached 90% and 10% comparing to the normal state resistance at 20 K. The variation of H_C as a function of temperature adheres to the relation of $1-(T/T_C)^2$ near T_C, as shown by the dotted line in Fig. 2(c). This tendency indicates that the patterned film well exhibits normal superconducting phenomena.

Fig. 3 also shows the resistance change as a function of temperature and magnetic field for the sample with the thickness of 100 nm. Transition behavior was clearly observed, showing systematic decrease of transition temperature with magnetic field in Fig. 3(a), which is similar with those of 400 nm thick film. In the value of T_C,

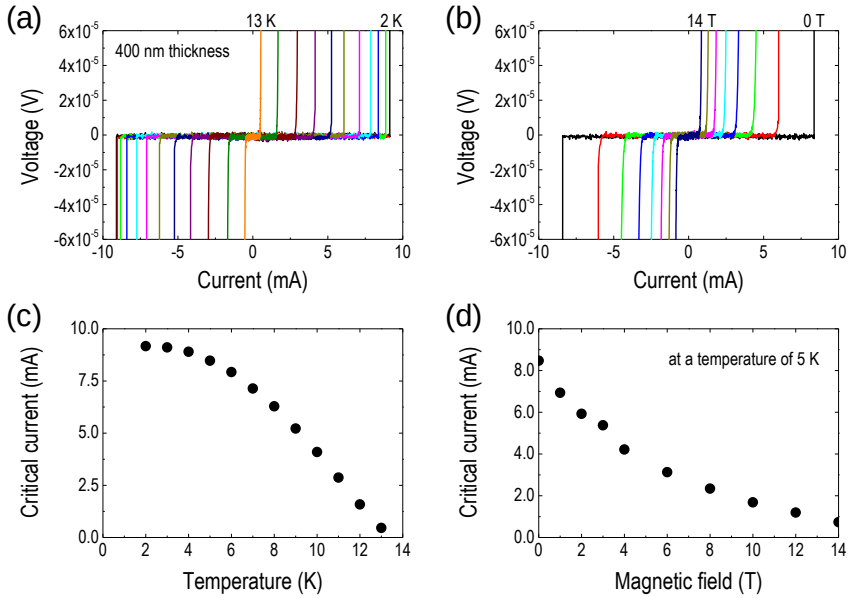

Fig. 4. Critical current of NbN-patterned film with a thickness of 400 nm. *I–V* characteristics at (a) various temperatures and (b) various magnetic fields. The critical current as a function of (c) temperature and (d) magnetic field. The critical current is defined as the value where the voltage becomes 5μV.

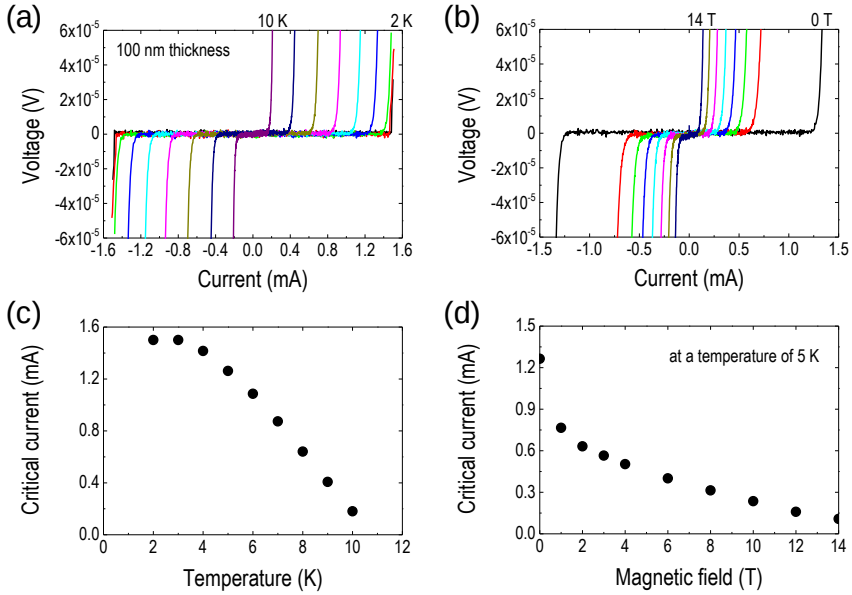

Fig. 5. Critical current of NbN-patterned film with a 100 nm thickness. *I–V* characteristics under (a) various temperatures and (b) various magnetic fields, respectively. The dependence of critical current on (c) temperature and (d) magnetic field, respectively.

however, the superconducting transition occurred at 11.4 K at 0 T which is lower than the corresponding value of 13.8 K for the sample with the thickness of 400 nm. This tendency also appeared under the magnetic field in Fig. 3(b) where the value of H_C became smaller. In addition, we can observe that the transition characteristics are somewhat broader than the thicker sample. Comparing Fig. 3(c) and Fig. 2(c), the temperature range (ΔT) between 90% and 10% resistance to normal resistance which indicates how rapidly the state changes from normal to superconducting state, is shown to increase when the thickness of NbN decreases. Nevertheless, the temperature dependence of H_C in the film with the thickness of 100 nm is also in a good agreement with $1-(T/T_C)^2$.

The zero-resistance characteristic means that current can flow without power loss. Thus, it is important to measure the current density in consideration of its application as a superconducting cable. Figs. 4 and 5 show the *I–V* characteristics of NbN patterned films with thickness of 400 nm and 100 nm, respectively. *I–V* curves were measured by changing the temperature at 0 T and by varying the magnetic field at a fixed temperature of 5 K. As shown in Figs. 4(a) and (b), as the

temperature and the intensity of the magnetic field become smaller, the superconductivity is maintained at higher currents, and the phase transition from the superconducting to the normal states is very sharp. The I_C is defined as the current value at the voltage of 5 μV. It can be expressed as a function of temperature and magnetic field, as shown in Figs. 4(c) and (d). The threshold current of the sample with the thickness of 400 nm is 9.17 mA at 2 K, which corresponds to 0.29 mA/cm2 in terms of J_C. In Fig. 4(c), the temperature dependence of the critical current shows a typical superconducting behavior, where I_C increases rapidly as the temperature decreases in the vicinity of T_C and becomes saturated far from T_C.

The voltage drop of a 100 nm thickness sample was measured as a function of the current under various temperatures and magnetic fields. The current range where voltage keeps zero gradually decreases with temperature increasing but appears a sharp decline even in the small magnetic field, as shown in Figs. 5(a) and (b). The superconducting breaking current at 2 K was measured to be equal to 1.5 mA and corresponded to a J_C of 0.16 mA/cm^2. The transition from the superconducting to the normal state occurs over rather broader range, which is consistent with the transition behavior of Fig. 3. However, because the characteristics of I_C in a 100 nm thickness sample can be comparable to those of the 400-nm thick sample as shown in Figs. 5(c) and (d), it seems that NbN films with thicknesses of 100 nm can also be utilized to make nano–micro patterned structures or hybrid structures with other functional materials. Nevertheless, it is necessary to optimize the conditions for better performance and for eliciting stable superconducting properties.

The NbN films deposited at 600 ℃ and 2 mTorr vacuum yielded excellent T_C and H_C values. However, the value of J_C is still smaller than those of other NbN thin films. When the T_C values of the samples with a thickness of 400 nm before and after the patterning process are compared, it is observed that the line-shaped sample has slightly lower transition temperature. It is plausible that crystallinity or morphology near the edges could be damaged during successive etching processes. As a result, we expect that the J_C of the as-grown NbN film will be higher. However, slight degradation does not impose drawbacks to our purpose because the overall superconducting properties have been well developed in the line-shaped NbN film.

4. CONCLUSIONS

The superconducting properties of sputter-deposited NbN thin films have been examined using the patterned line-shaped samples by Ar RIE process on a SiO_2/Si substrate. The superconducting transition temperature varied within the range of 13 K and 15 K for films with thicknesses of 100 nm to 400 nm. Based on the critical magnetic fields and critical current densities at various temperatures, the properties of the sample with a thickness of 100 nm in comparison to those of a sample with a thickness of 400 nm showed some degradation which may come from the substantial surface effect in the thinner samples. In spite of reduction of critical values, however, the overall superconducting characteristics are well preserved, which supports NbN thin film with various thicknesses can be used in the systems which require superconductivity. In addition, the narrower line-shaped device needs to be explored in the future on the basis of the understanding of the superconducting properties, as described and analyzed in this study.

ACKNOWLEDGMENT

This work was supported by a 2-Year Research Grant of Pusan National University.

REFERENCES

[1] D. Dochev, V. Desmaris, A. Pavolotsky, D. Meledin, Z. Lai, *et al.*, "Growth and characterization of epitaxial ultra-thin NbN films on 3C-SiC/Si substrate for terahertz applications," *Supercond. Sci. Technol.*, Vol. 24, pp. 035016, 2011.

[2] F. Marsili, A. Gaggero, L. H. Li, A. Surrente, R. Leoni, *et al.*, "High quality superconducting NbN thin films on GaAs," *Supercond. Sci. Technol.*, Vol. 22, pp. 095013, 2009.

[3] P. Khosropanah, J. R. Gao, W. M. Laauwen, M. Hajenius and T. M. Klapwijk, "Low noise NbN hot electron bolometer mixer at 4.3THz," *Appl. Phys. Lett.*, Vol. 91, pp. 221111, 2007.

[4] Y. Nakamura, H. Terai, K. Inomata, T. Yamamoto, W. Qiu, *et al.*, "Superconducting qubits consisting of epitaxially grown NbN/AlN/NbN Josephson junctions," *Appl. Phys. Lett.*, Vol. 99, pp. 212502, 2011.

[5] R. Sanjinés, M. Benkahoul, M. Papagno, F. Lévy and D. Music, "Electronic structure of Nb2N` NbN thin films," *J. Appl. Phys.*, Vol. 99, pp. 044911, 2006.

[6] G. i. Oya and Y. Onodera, "Phase transformations in nearly stoichiometric NbNx," *J. Appl. Phys.*, Vol. 47, pp. 2833-2840, 1976.

[7] A. E. Dane, *Reactive DC magnetron sputtering of ultrathin superconducting niobium nitride films*. Massachusetts Institute of Technology, 2015.

[8] T. Shiino, S. Shiba, N. Sakai, T. Yamakura, L. Jiang, *et al.*, "Improvement of the critical temperature of superconducting NbTiN and NbN thin films using the AlN buffer layer," *Supercond. Sci. Technol.*, Vol. 23, pp. 045004, 2010.

[9] A. Bhat, X. Meng, A. Wong and T. Van Duzer, "Superconducting NbN films grown using pulsed laser deposition for potential application in internally shunted Josephson junctions," *Supercond. Sci. Technol.*, Vol. 12, pp. 1030-1032, 1999.

[10] G. Saraswat, P. Gupta, A. Bhattacharya and P. Raychaudhuri, "Highly oriented, free-standing, superconducting NbN films growth on chemical vapor deposited graphene," *APL Mater.*, Vol. 2, pp. 056103, 2014.

[11] W. M. Roach, J. R. Skuza, D. B. Beringer, Z. Li, C. Clavero, *et al.*, "NbN thin films for superconducting radio frequency cavities," *Supercond. Sci. Technol.*, Vol. 25, pp. 125016, 2012.

[12] T. Yamashita, K. Hamasaki, Y. Kodaira and T. Komata, "Nano-meter bridge with epitaxially deposited NbN on MgO film," *IEEE Trans. Magn.*, Vol. 21, pp. 932-934, 1985.

[13] M. Ukibe and G. Fujii, "Superconducting Characteristics of NbN Films Deposited by Atomic Layer Deposition," *IEEE Trans. Appl. Supercond.*, Vol. 27, pp. 1-4, 2017.

[14] D. Hazra, N. Tsavdaris, S. Jebari, A. Grimm, F. Blanchet, *et al.*, "Superconducting properties of very high quality NbN thin films grown by high temperature chemical vapor deposition," *Supercond. Sci. Technol.*, Vol. 29, pp. 105011, 2016.

[15] G. Zou, M. Jain, H. Zhou, H. Luo, S. A. Baily, *et al.*, "Ultrathin epitaxial superconducting niobium nitride films grown by a chemical solution technique," *Chem. Commun. (Camb.)*, Vol. pp. 6022-6024, 2008.

[16] J. R. Gao, M. Hajenius, F. D. Tichelaar, T. M. Klapwijk, B. Voronov, *et al.*, "Monocrystalline NbN nanofilms on a 3C-SiC/Si substrate," *Appl. Phys. Lett.*, Vol. 91, pp. 062504, 2007.

[17] S. H. Bedorf, *Development of ultrathin niobium nitride and niobium titanium nitride films for THz hot-electron bolometers*. Universität zu Köln, 2005.

[18] C. Delacour, B. Pannetier, J. C. Villegier and V. Bouchiat, "Quantum and thermal phase slips in superconducting niobium nitride (NbN) ultrathin crystalline nanowire: application to single photon detection," *Nano Lett.*, Vol. 12, pp. 3501-3506, 2012.

[19] O. Kahl, S. Ferrari, V. Kovalyuk, G. N. Goltsman, A. Korneev, *et al.*, "Waveguide integrated superconducting single-photon detectors with high internal quantum efficiency at telecom wavelengths," *Sci. Rep.*, Vol. 5, pp. 10941, 2015

[20] C. M. Natarajan, M. G. Tanner and R. H. Hadfield, "Superconducting nanowire single-photon detectors: physics and applications," *Supercond. Sci. Technol.*, Vol. 25, pp. 063001, 2012.

[21] J. A. O'Connor, M. G. Tanner, C. M. Natarajan, G. S. Buller, R. J. Warburton, *et al.*, "Spatial dependence of output pulse delay in a niobium nitride nanowire superconducting single-photon detector," *Appl. Phys. Lett.*, Vol. 98, pp. 201116, 2011.

[22] P. Rath, O. Kahl, S. Ferrari, F. Sproll, G. Lewes-Malandrakis, *et al.*, "Superconducting single-photon detectors integrated with diamond nanophotonic circuits," *Light Sci. Appl.*, Vol. 4, pp. e338, 2015.

[23] D. H. Youn, G. Bae, S. Han, J. Y. Kim, J.-W. Jang, *et al.*, "A highly efficient transition metal nitride-based electrocatalyst for oxygen reduction reaction: TiN on a CNT–graphene hybrid support," *J. Mater. Chem. A*, Vol. 1, pp. 8007-8015, 2013.

[24] J.-G. Kim, H. Kang, Y. Lee, J. Park, J. Kim, *et al.*, "Carbon-Nanotube-Templated, Sputter-Deposited, Flexible Superconducting NbN Nanowire Yarns," *Adv. Funct. Mater.*, Vol. 27, pp. 1701108, 2017.

[25] Z. Feng, J. Yuan, G. He, W. Hu, Z. Lin, *et al.*, "Tunable critical temperature for superconductivity in FeSe thin films by pulsed laser deposition," *Sci. Rep.*, Vol. 8, pp. 4039, 2018.

[26] R. Jha and V. Awana, "Control of sputtering parameters for deposition of NbN thick films," *Novel Supercond. Mater.*, Vol. 1, pp. 7-12, 2015.